New Journal of Physics
The open access journal at the forefront of physics

Deutsche Physikalische Gesellschaft DPG
IOP Institute of Physics

Published in partnership with: Deutsche Physikalische Gesellschaft and the Institute of Physics

OPEN ACCESS

RECEIVED
5 May 2018

REVISED
4 December 2018

ACCEPTED FOR PUBLICATION
16 January 2019

PUBLISHED
31 January 2019

PAPER

Biexciton as a Feshbach resonance and Bose–Einstein condensation of paraexcitons in Cu_2O

Cam Ngoc Hoang

Institute of Physics, Vietnam Academy of Science and Technology, No 10 Dao Tan St, 118000 Hanoi, Vietnam

E-mail: hncam@iop.vast.ac.vn

Keywords: condensed matter theory, two-channel scattering, feshbach resonance, paraexciton loss in Cu_2O, quasibiexciton, spin-dependent exciton–exciton interaction, Bose–Einstein condensation of excitons

Supplementary material for this article is available online

Abstract

Paraexcitons, the lowest energy exciton states in Cu_2O, have been considered a good system for realizing exciton Bose–Einstein condensation (BEC). The fact that their BEC has not been attained so far is attributed to a collision-induced loss, whose nature remains unclear. To understand collisional properties of cold paraexcitons governing their BEC, we perform a theoretical analysis of the s-wave paraexciton–paraexciton scattering at low temperatures. We show the two-channel character of the scattering, where incoming paraexcitons are coupled to a biexciton in a closed channel. Being embedded in the paraexciton scattering continuum, the biexciton is a Feshbach resonance giving rise to a paraexciton loss and a diminution of their background scattering length. In strain-induced traps, the biexciton effects generally increase with stress. Thus the scattering length a of trapped paraexcitons decreases monotonically with stress turning its sign as stress goes beyond a critical value. In the stress range with $a < 0$, the paraexciton loss increases with stress, whereas in that with $a > 0$ the loss is almost stress-independent. Importantly, that in the latter case the loss rate can be reduced to such small values that it has no effects on BEC by lowering temperatures to near one Kelvin and below. Our approximate calculations give the critical value of stress in the range just above one kilobar; thus BEC of strain-confined paraexcitons might be attained under low stress at a subkelvin temperature.

Introduction

Exciton in semiconductors is a Coulomb-bound pair of an electron in the conduction band and a hole in the valence band. In the low-density limit, excitons behave as bosons, so they may undergo Bose–Einstein condensation (BEC) if their lifetime is long enough to allow the system to reach quasiequilibrium [1–3]. Therefore BEC is expected in Cu_2O where the dipole-forbidden 1s excitons of the yellow series have a relatively long lifetime. The internal electron–hole exchange splits the state into the nondegenerate paraexciton and higher lying triply degenerate orthoexciton, separated by an energy of $\Delta = 12$ meV [4]. The orthoexciton is quadruply allowed, while the paraexciton is strictly forbidden resulting in its particularly long lifetime [5]. Owing to this unique property and also to their large binding energy, paraexcitons in Cu_2O have long been considered a good system to realize exciton BEC.

Much effort has been made during the past several decades, but compelling evidence of BEC in Cu_2O has not been obtained [6–14]. A collisional loss is believed to prevent the paraexciton density from being as high as necessary for BEC [7, 12–18], but an established understanding of the process is still lacking [19]. The loss rate has been found to increase with stress in strain-induced harmonic traps [16], which are needed to avoid paraexciton heating and diffusion as well as to lower the critical density [7, 20, 21]. Thus experiments lately have been conducted with moderate stress at subkelvin temperatures involving low critical densities [10–13]. An 'explosion', however, was observed when the critical density was attained for trapped paraexcitons [10, 11]. The loss is conventionally attributed to Auger recombination, but its nature has not been elucidated [19, 22]. Later, the participation of a biexciton [23, 24] and an inelastic collision of paraexcitons [18] have been suggested, but

their microscopic mechanisms are still open for making clear. In general, despite the recent experimental progress toward paraexciton BEC [10–13], a fundamental issue of the problem—the interparticle interaction remains unsolved.

To understand and possibly to control obstacles to attaining paraexciton BEC, in this paper we perform a microscopic description of the paraexciton–paraexciton scattering at low temperatures. We begin by formulating the Hamiltonian of a closed paraexciton system starting from its original electron–hole picture. This enables us to establish the interconversion between a pair of paraexcitons and that of orthoexcitons, which results in the two-channel character of the paraexciton–paraexciton scattering. To obtain salient features of the s-wave collision dominating the scattering at low temperatures, we develop an approximate way of dealing with the nonlocal exchange part of interaction potentials in two channels, which is also the coupling potential. This makes it possible for us to estimate the paraexciton background scattering length, the binding energy and envelope function of a biexciton supported by the closed channel as well as the strength of the coupling between the biexciton and paraexciton scattering states. With this coupling, the biexciton is not a bound state that can be detected, but a Feshbach resonance that manifests itself through changes it causes in collisional properties of paraexcitons. The resonance gives rise to a paraexciton loss and an extra attractive interaction joining up with the background paraexciton–paraexciton repulsive interaction, which are generally enhanced with increasing stress in strain-induced traps. As a result, the scattering length a of trapped paraexcitons turns negative as stress goes beyond a critical value S_0. In the stress range $S < S_0$, where $a > 0$, the paraexciton loss rate is almost stress-independent, whereas in the range $S > S_0$ it increases with stress. The former case is suitable for BEC due to the repulsive two-body interaction among paraexcitons as well as the possibility to reduce the loss rate to harmless for BEC values. In fact, we find for a temperature near one Kelvin that the loss rate under stress $S < S_0$ is more than one order of magnitude less than the critical value above which BEC is impossible [19]. The loss rate, which is proportional to the paraexciton-phonon scattering rate, decreases still with temperature decreasing into the subkelvin range. For the averaged value of the hole-to-exciton mass ratio corresponding to the accepted values of the key exciton parameters, we find S_0 in the range just above one kilobar. This suggests that the explosion reported in [10] may be connected with the negative scattering length of strain-confined paraexcitons under moderate stress. Thus our results offer an interpretation of a number of experimental observations and suggest that experiments on paraexciton BEC should be performed under low stress at a subkelvin temperature.

Results

Two-channel nature of paraexciton–paraexciton scattering

We use the second quantization formalism for an elucidation of the effective spin-dependent two-body interaction among paraexcitons. We start from the fact that excitons are long-live quasiparticles introduced for an effective description of electron–hole-pair systems with their inherent many-body Coloumb-mediated correlations. Each exciton is 'dressed' by the Coulomb attraction of an electron with a hole and related to the other ones by the 'residual' interaction that comes from the remaining part of the many-body correlations. As regards the yellow-series 1s exciton in the Cu_2O crystal with full cubic symmetry, we consider it in the simple two-band model neglecting the fine effects connected with the interaction of the valence band Γ_7^+ with the lower lying valence band Γ_8^+ [25]. In such an approximation the exciton is formed from electrons of the lowest conduction band Γ_6^+ and holes of the highest valence band Γ_7^+, both having effective spin 1/2. According to the group-theoretical expansion,

$$\Gamma_1^+ \otimes \Gamma_6^+ \otimes \Gamma_7^+ = \Gamma_2^+ \oplus \Gamma_5^+, \tag{1}$$

it splits into the nondegenerate paraexciton Γ_2^+ with angular momentum $J = 0$ and the orthoexciton Γ_5^+ with $J = 1$. Here the unit representation Γ_1^+ characterizes symmetry of the 1s hydrogenlike function describing the electron and hole relative motion in the exciton. The relationship between basis functions of the irreducible representations of a direct product and of those the product expanded into [26] give us

$$P_{\mathbf{k}}^+ \mid \mathbf{0}\rangle = \frac{1}{\sqrt{V}}\sum_{\mathbf{p}} \mathsf{F}(\mathbf{p} - \beta\mathbf{k})\frac{1}{\sqrt{2}}(e^+_{1/2,\mathbf{k}-\mathbf{p}}h^+_{-1/2,\mathbf{p}} + e^+_{-1/2,\mathbf{k}-\mathbf{p}}h^+_{1/2,\mathbf{p}})\mid 0\rangle, \tag{2}$$

$$O^+_{M\mathbf{k}} \mid \mathbf{0}\rangle = \frac{1}{\sqrt{V}}\sum_{\mathbf{p}} \mathsf{F}(\mathbf{p} - \beta\mathbf{k}) \times \begin{cases} e^+_{1/2,\mathbf{k}-\mathbf{p}}h^+_{1/2,\mathbf{p}}\mid 0\rangle, & M = 1, \\ \frac{1}{\sqrt{2}}(e^+_{1/2,\mathbf{k}-\mathbf{p}}h^+_{-1/2,\mathbf{p}} - e^+_{-1/2,\mathbf{k}-\mathbf{p}}h^+_{1/2,\mathbf{p}})\mid 0\rangle, & M = 0, \\ e^+_{-1/2,\mathbf{k}-\mathbf{p}}h^+_{-1/2,\mathbf{p}}\mid 0\rangle, & M = -1, \end{cases} \tag{3}$$

where $\mid 0\rangle$ is the semiconductor ground state, $\mid \mathbf{0}\rangle$—that state mapped on the space of excitons, $P_{\mathbf{k}}^+\mid 0\rangle$—the momentum $\mathbf{k}$ paraexciton state, $O^+_{M\mathbf{k}}\mid 0\rangle$—that of the orthoexciton ($M = -1,0,1$ is the projection of the orthoexciton angular momentum on the quantization axis), and $e^+_{\sigma_e,\mathbf{p}_e}h^+_{\sigma_h,\mathbf{p}_h}\mid 0\rangle$ stands for a correlated electron–hole

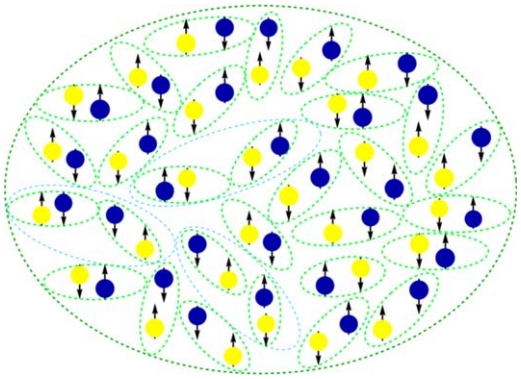

Figure 1. Ensemble of correlated electron–hole pairs that constitutes a closed paraexciton system. Small blue (yellow) balls with arrows depict electrons (holes) with spin-up and spin-down. Dashed light-blue ovals confine correlated two-pair structures with different spin combinations that constitute two correlated paraexcitons.

pair with total spin projection $\sigma_e + \sigma_h$ and total momentum $\mathbf{p}_e + \mathbf{p}_h$. Here $e^+_{\sigma,\mathbf{p}}$ ($h^+_{\sigma,\mathbf{p}}$) denotes the creation operator of an electron (a hole) with spin projection σ ($\sigma = 1/2$ for spin-up and $\sigma = -1/2$ spin-down) and momentum $\mathbf{p}$. In equations (2) and (3) V is the sample volume, $\mathrm{F}(\mathbf{p} - \beta\mathbf{k})$—the 1$s$ exciton envelope function in the momentum space with $\beta = \mu_h/\mu_x$ the hole-to-exciton mass ratio ($\mu_x = \mu_e + \mu_h$), and the particular values of Clebsh–Gordan coefficients are taken from the tables of Clebsh–Gordan coefficients relevant to irreducible representations of the O_h group [27].

Taking into account the fact, that in relevant experiments only 1s excitons are excited, we have the relationship between correlated electron–hole pairs and excitons inverse to equations (2) and (3)

$$\begin{aligned}
e^+_{1/2,\mathbf{k}_e} h^+_{1/2,\mathbf{k}_h}|\,0\,\rangle &= \frac{1}{\sqrt{V}}\mathrm{F}(\alpha\mathbf{k}_h - \beta\mathbf{k}_e) O^+_{1,\mathbf{k}_e+\mathbf{k}_h}|\,0\,\rangle,\\
e^+_{1/2,\mathbf{k}_e} h^+_{-1/2,\mathbf{k}_h}|\,0\,\rangle &= \frac{1}{\sqrt{2V}}\mathrm{F}(\alpha\mathbf{k}_h - \beta\mathbf{k}_e)(P^+_{\mathbf{k}_e+\mathbf{k}_h} + O^+_{0,\mathbf{k}_e+\mathbf{k}_h})|\,0\,\rangle,\\
e^+_{-1/2,\mathbf{k}_e} h^+_{1/2,\mathbf{k}_h}|\,0\,\rangle &= \frac{1}{\sqrt{2V}}\mathrm{F}(\alpha\mathbf{k}_h - \beta\mathbf{k}_e)(P^+_{\mathbf{k}_e+\mathbf{k}_h} - O^+_{0,\mathbf{k}_e+\mathbf{k}_h})|\,0\,\rangle,\\
e^+_{-1/2,\mathbf{k}_e} h^+_{-1/2,\mathbf{k}_h}|\,0\,\rangle &= \frac{1}{\sqrt{V}}\mathrm{F}(\alpha\mathbf{k}_h - \beta\mathbf{k}_e) O^+_{-1,\mathbf{k}_e+\mathbf{k}_h}|\,0\,\rangle.
\end{aligned} \tag{4}$$

Assuming the ortho-para conversion in a real experiment at low temperatures to be instantaneous, we consider a closed paraexciton system, which actually includes ensembles of zero-spin correlated electron–hole pairs. A schematic representation of such an ensemble is shown in figure 1. The residual interaction among paraexcitons arises from correlations between the electron and hole of each pair with all the electrons and holes of the other pairs, which are governed by the Coulomb forces and Pauli exclusion principle of indistinguishability. It includes two-body, three-body, and higher multi-body interactions, among which in dilute conditions the two-body interaction dominates. There exist several ways of deriving an exciton Hamiltonian with two-body effective interaction from that of the original electron–hole system [28–32]. In our previous work [33], we have done this for the common case of direct-gap two-band semiconductors by adopting the bosonization approach of Hanamura [28, 29] with the particles spin taken into consideration. The approach can be justified as follows. When one electron–hole pair is present in the system, the internal pair correlation (Coulomb attraction) binds the electron and hole into an exciton. The binding energy and size of the exciton are expressed in terms of the exciton Rydberg energy R_x and effective radius $_{ax}$, respectively. Being the energy and length scales of the internal pair correlation, these quantities present a physical property of the semiconductor. Strictly speaking, only in this hypothetical case of one pair in the system the exciton is an ideal (noninteracting) boson. Already when there are two pairs, two-pair correlations produce qualitative changes. In dynamical respect, being mediated by interpair Coulomb forces, these correlations give rise to the exciton–exciton interaction of the order of $R_x na_x^3$, while in statistical aspect, they make excitons deviate from bosons by adding a non-bosonic correction of the order of na_x^3 [3]. Here n=N/V (N is the number of electron–hole pairs) is the density of pairs in the system. When there are more pairs, three-pair and higher multi-pair correlations lead to three-exciton and higher multi-exciton interactions, whose scale is, respectively, $R_x(na_x^3)^2$ and corresponding higher orders of na_x^3 multiplied by R_x. When n is so small that na_x^3 is an infinitesimal quantity, one can consider only the internal correlation inside pairs. A system of N pairs is represented in the exciton space by that of N noninteracting excitons-bosons, which are the eigenstates of the exciton system's Hamiltonian in the linear

approximation. In the low-density limit, wherein na_x^3 is very small, $na_x^3 \ll 1$, but finite, one has to consider the effect of two-pair correlations. To do this, in the exciton-boson approach the system of excitons-bosons is used as an orthonormal basis for representing Coulomb-mediated two-pair correlations in the form of the effective exciton–exciton interaction. Certainly, such an approach does not allow to describe both the exciton–exciton interaction and their non-bosonic nature at the same time [34]. Therefore it is applicable only for the low-density limit that is under consideration in this paper. Combined effects of the two consequences of two-pair correlations, which are of the order of $R_x(na_x^3)^2$ as those of three-pair correlations, have to be taken into consideration when n_{ax}^3 is not very small. However, that is beyond the scope of the paper.

Thus, using the bosonization approach of Hanamura, we map correlations among the constituents of two zero-spin correlated electron–hole pairs, which can be in three possible spin combinations as structures marked by light-blue ovals in figure 1, onto the exciton space to obtain the Hamiltonian

$$\begin{aligned} H_{p-p} = &\sum_{\mathbf{k}} E_p(k) P_{\mathbf{k}}^+ P_{\mathbf{k}} + \sum_{\mathbf{k}} E_o(k) \sum_{M=-1,0,1} O_{M,\mathbf{k}}^+ O_{M,\mathbf{k}} \\ &+ \frac{1}{2V} \sum_{\mathbf{k}_1,\mathbf{k}_2,\mathbf{q}} \{U^d(q) O_{1,\mathbf{k}_1+\mathbf{q}}^+ O_{-1,\mathbf{k}_2-\mathbf{q}}^+ O_{-1,\mathbf{k}_2} O_{1,\mathbf{k}_1} \\ &+ \left[U^d(q) + \frac{1}{2}U^{\mathrm{ex}}(\mathbf{k}_1 - \mathbf{k}_2, \mathbf{q})\right][P_{\mathbf{k}_1+\mathbf{q}}^+ P_{\mathbf{k}_2-\mathbf{q}}^+ P_{\mathbf{k}_2} P_{\mathbf{k}_1} + O_{0,\mathbf{k}_1+\mathbf{q}}^+ O_{0,\mathbf{k}_2-\mathbf{q}}^+ O_{0,\mathbf{k}_2} O_{0,\mathbf{k}_1}] \\ &- \frac{1}{2}U^{\mathrm{ex}}(\mathbf{k}_1 - \mathbf{k}_2, \mathbf{q})[(O_{1,\mathbf{k}_1+\mathbf{q}}^+ O_{-1,\mathbf{k}_2-\mathbf{q}}^+ + O_{-1,\mathbf{k}_1+\mathbf{q}}^+ O_{1,\mathbf{k}_2-\mathbf{q}}^+) O_{0,\mathbf{k}_2} O_{0,\mathbf{k}_1} + \mathrm{h.c.}] \\ &+ \frac{1}{2}U^{\mathrm{ex}}(\mathbf{k}_1 - \mathbf{k}_2, \mathbf{q})[(O_{1,\mathbf{k}_1+\mathbf{q}}^+ O_{-1,\mathbf{k}_2-\mathbf{q}}^+ + O_{-1,\mathbf{k}_1+\mathbf{q}}^+ O_{1,\mathbf{k}_2-\mathbf{q}}^+ + O_{0,\mathbf{k}_1+\mathbf{q}}^+ O_{0,\mathbf{k}_2-\mathbf{q}}^+) P_{\mathbf{k}_2} P_{\mathbf{k}_1} \\ &+ \mathrm{h.c.}]\}, \end{aligned} \tag{5}$$

where $E_p(k)$ and $E_o(k)$ denote the paraexciton and orthoexciton energy, respectively, U^d and U^{ex} are energy densities of the direct and exchange exciton–exciton interaction [28, 32], and h.c. stands for hermitian conjugates. The last two terms in the curly brackets show that the exchange interaction can flip the spin of interacting excitons. It either turns two longitudinal orthoexcitons ($M = 0$) to a pair of transverse ones with opposite orientations of the angular momentum ($M = 1, -1$), or convert a paraexciton pair to a pair of orthoexcitons, and vice versa. Here in this paper, the term orthoexcitons is used to refer exclusively to the ones that go in pair with zero total angular momentum. As $U^{\mathrm{ex}} > 0$ [28, 30], we see that the two-body interaction in a paraexciton system is generally repulsive except for the case of the spin-flip exchange interaction between two orthoexcitons, which is attractive. Although the form of the attractive exchange exciton–exciton interaction is different in different semiconductors depending on their particular symmetry, the common fact is the attraction arises exclusively from exchange correlations between distinguished pairs. In the case under consideration, let us pay attention to the three two-pair complexes with different spin combinations that constitute two correlated paraexcitons. One can see that the complex depicted in figure 2(a) is unique in the sense that it does not contains identical carriers-fermions, while the ones in figure 2(b) do. Being subject to the Pauli exclusion principle, the two identical electrons and holes inside the complexes in figure 2(b) repel each other at distances, where their wave functions overlap. This results in the repulsive exchange interaction between paraexcitons and longitudinal orthoexcitons with each other as well as among themselves. Concerning the complex in figure 2(a), the principle Pauli does not apply to its carriers. The four members are on equal footing, so they prefer to stay together in the totally symmetric complex by an attractive interaction. In Cu_2O with O_h crystal symmetry, however, the repulsion between the orthoexciton and paraexciton that arises from the internal exchange predominates. Consequently, as we see from figure 2(a), the spin-flip exchange interaction of a pair of transverse orthoexcitons into longitudinal orthoexcitons is attractive, while that into paraexcitons is repulsive.

Thus, with the effective two-body interaction taken into consideration, a 'paraexciton system' theoretically incorporates not only paraexcitons but also orthoexcitons that go in pairs. In this connection, neither the states of paraexciton pairs nor those of orthoexciton pairs can form eigenstates of Hamiltonian (5). They form just components, or substates of eigenstates, which have the form of two-exciton vectors with definite momentum

$$\begin{aligned} \Psi_{p-p}(\mathbf{K}) = \frac{1}{\sqrt{2V}} \sum_{\mathbf{s}} \Big[&\psi_{pp}(\mathbf{s}) P_{\mathbf{s}+\mathbf{K}/2}^+ P_{-\mathbf{s}+\mathbf{K}/2}^+ + \frac{1}{\sqrt{3}} \psi_{po}(\mathbf{s}) (O_{0,\mathbf{s}+\mathbf{K}/2}^+ O_{0,-\mathbf{s}+\mathbf{K}/2}^+ \\ &O_{-1,\mathbf{s}+\mathbf{K}/2}^+ O_{1,-\mathbf{s}+\mathbf{K}/2}^+ + O_{1,\mathbf{s}+\mathbf{K}/2}^+ O_{-1,-\mathbf{s}+\mathbf{K}/2}^+) \Big] |0\rangle, \end{aligned} \tag{6}$$

where ψ_{pp} and ψ_{po} are envelope functions, respectively, of 'bare' paraexciton and orthoexciton pairs. The Schrodinger equation $H_{p-p}\Psi_{p-p}(\mathbf{K}) = E_{p-p}(K)\Psi_{p-p}(\mathbf{K})$ leads to a system of equations for ψ_{pp} and ψ_{po}

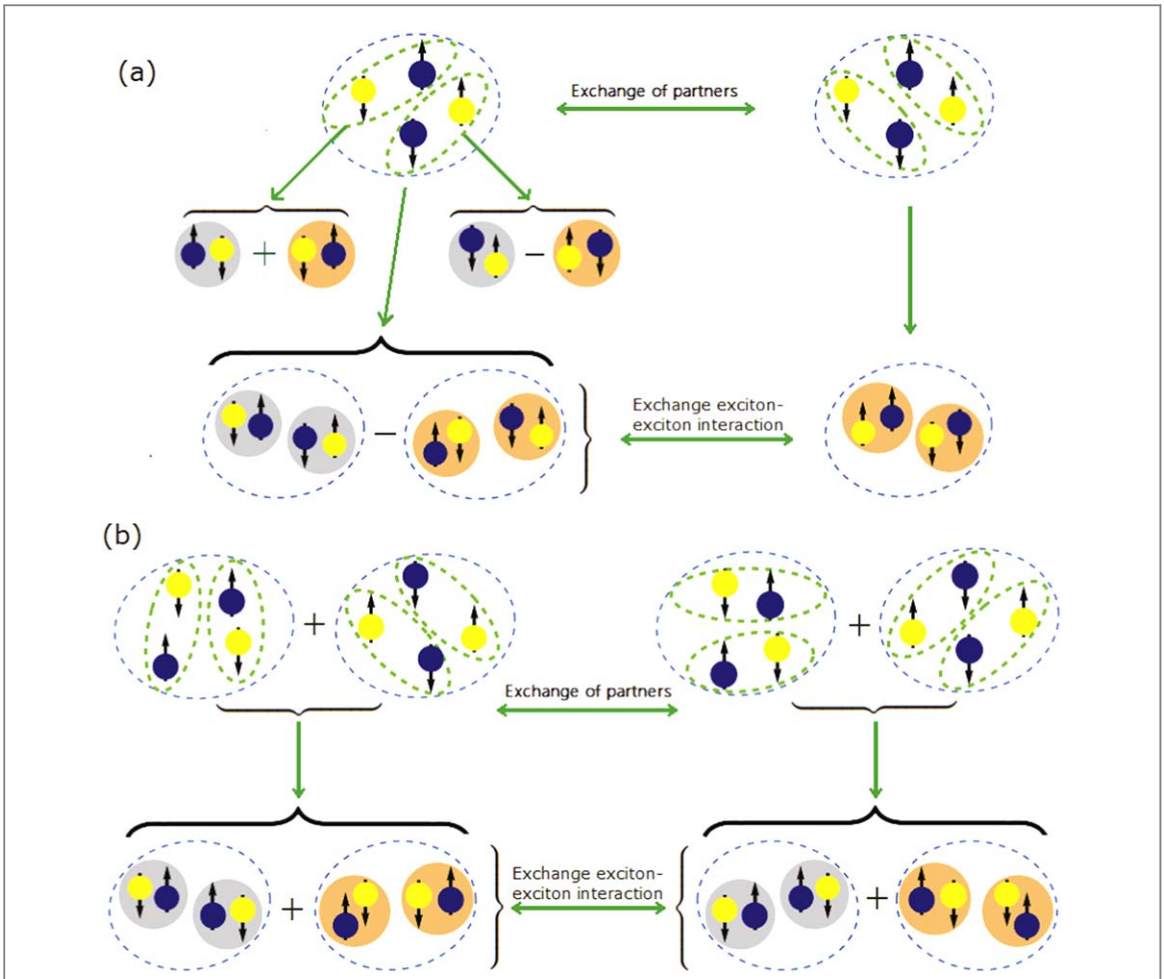

Figure 2. Mechanism of the exchange exciton–exciton interaction. Grey (orange) balls denote the dark paraexciton (bright orthoexcitons) with the angular momentum projection equal to the sum of those of the constituent electron and hole. (a) Left: on the top is one of three complexes of two correlated electron–hole pairs that constitute two correlated paraexcitons. The complex includes two different pairs, so all four particles are distinguished. Each correlated pair is represented in the exciton space by a linear combination of a paraexciton and a longitudinal orthoexciton in accordance with equation (4). As a result, the whole complex is represented by a combination of a correlated pair of paraexcitons and that of longitudinal orthoexcitons. Right: the two-pair complex on the top is obtained from the one on the left by an exchange of partners between two pairs. It is represented in the exciton space by a pair of correlated transverse orthoexcitons with opposite orientations of the angular momentum. Thus, the exchange correlations between two distinguished electron–hole pairs are reproduced in the exciton space by the spin-flip mutual interaction of paraexcitons and longitudinal orthoexcitons into a pair of transverse orthoexcitons; the former is repulsive, while the latter is attractive. Two-side arrows allow to read the schema from right to left when it represents the reverse process. (b) The same description as in (a) for two other complexes.

$$
\begin{aligned}
&-\left(\frac{\hbar^2 s^2}{\mu_x}+E\right)\psi_{pp}(\mathbf{s})+\frac{1}{V}\sum_{\mathbf{q}}\left[U^d(\mathbf{q})+\frac{1}{2}U^{\mathrm{ex}}(2\mathbf{s},\mathbf{q})\right]\psi_{pp}(\mathbf{s}+\mathbf{q})\\
&+\frac{\sqrt{3}}{2V}\sum_{\mathbf{q}}U^{\mathrm{ex}}(2\mathbf{s},\mathbf{q})\psi_{po}(\mathbf{s}+\mathbf{q})=0,\\
&\left(-\frac{\hbar^2 s^2}{\mu_x}+2\Delta-E\right)\psi_{po}(\mathbf{s})+\frac{1}{V}\sum_{\mathbf{q}}\left[U^d(\mathbf{q})-\frac{1}{2}U^{\mathrm{ex}}(2\mathbf{s},\mathbf{q})\right]\psi_{po}(\mathbf{s}+\mathbf{q})\\
&+\frac{\sqrt{3}}{2V}\sum_{\mathbf{q}}U^{\mathrm{ex}}(2\mathbf{s},\mathbf{q})\psi_{pp}(\mathbf{s}+\mathbf{q})=0,
\end{aligned}
\tag{7}
$$

where μ_x is assumed the same for both types of the exciton and $E = k_B T$ (k_B is the Boltzmann constant, T—the temperature)—paraexciton thermal energy. With the paraexciton scattering threshold chosen as the energy zero, E is the relative energy of colliding paraexcitons at large distances, where their mutual interaction disappears. Since $E > 0$, the interaction potential between paraexcitons forms the energetically open channel, also called entrance or background channel. It is coupled by the exchange exciton–exciton interaction potential to a channel formed by the interaction potential between orthoexcitons. Being situated higher than the paraexciton scattering threshold by 2Δ, the latter is a closed channel for the paraexciton scattering at any energy

$E < 2\Delta$. With such energy, paraexcitons can exit in the open channel after their collision, but not in the closed channel. Salient features of the paraexciton–paraexciton scattering can be drawn from equation (7) in the case the coupling and interaction potentials are defined. These potentials incorporate the exchange exciton–exciton interaction potential, whose description is a long-standing problematic issue of exciton physics. That is connected with its nonlocality, which always presents in the case when real interactions in a many-particle system are described in terms of an effective interaction between quasiparticles. The potential depends at any point on the wave function everywhere in a surrounding region, whose range coincides with its range. Therefore, coupled equation (7) form a system of integro-differential equations in the coordinate space, which cannot be analyzed with usual methods of nonlinear dynamics. Thus we are forced to make approximations from the outset. First, we limit ourselves to the s-wave paraexciton–paraexciton collision at such temperatures, that $E \ll 2\Delta$, which we refer to as low temperatures. In this case, the probability of the para-ortho up-conversion is practically zero and the influence of the closed channel on the paraexciton scattering can be treated by perturbation theory [26]. In the first approximation (the zeroth order in perturbation) the scattering is described by two uncoupled channels obtained from equation (7) by leaving aside the coupling terms. Since the first order correction is zero, the next approximation is of the second order in perturbation.

Approximate interaction potentials and solutions for bare channels

We need to define interaction and coupling potentials for the case of the s-type envelope functions in bare channels. All we have is a presentation of the direct and exchange interaction density U^d and $U^{\rm ex}$ in the form of averages of the screened Coulomb potential $U_{\rm cl}(p) \propto e^2/\epsilon p^2$ (e is the elementary charge and ϵ—the dielectric constant) over the states of two excitons before and after the interaction. Generally, we can obtain an integral presentation for the direct and exchange interaction potentials from U^d and $U^{\rm ex}$ by retransforming $U_{\rm cl}(q)$ and the exciton wave function F, which depends parametrically on mass ratios β and $\alpha = 1 - \beta$, to the position space [35]. For the yellow-series 1s exciton in Cu_2O with its effective radius $_{ax}$ comparable to the lattice constant a_l, central cell corrections [36] cause complexity. By producing a momentum dependence of ϵ and of the exciton effective mass involving that of β, these corrections make the inverse Fourier transformation difficult. Especially, that is impracticable for function F because the dependence of β on momentum, which is connected yet with nonparabolicity of the Γ_7^+ valence band [37], is hard to establish. We have to resort to approximations to capture essential features of the exciton–exciton interaction potential. We note that, the first momentum-correction to ϵ adds to the direct and exchange interaction potentials a respective extra potential that is more than two orders of magnitude weaker (that is $(\epsilon/\mathrm{d})(a_x/a_l)^2 \gtrsim 10^2$ with $d \approx 0.18$ [36]). Therefore in dealing with U^d and $U^{\rm ex}$ we can neglect the momentum correction and treat ϵ as a constant as well as put the Coulomb prefactor e^2/ϵ equal to $2E_b a_x$, E_b is the exciton experimental binding energy. In that case, to a set of values of the key exciton parameters E_b, $_{ax}$, and μ_x, there corresponds an averaged value of β according to relations $\mu_r/\mu_x = (1 - \beta)\beta$ and $\hbar^2/2\mu_r = E_b a_x^2$. With the constant β, the direct part of interaction potentials in bare channels is calculated in a closed analytical form showing that it matters only at distances $r \lesssim {}_{ax}$ [35]. Concerning the exchange part, the formula for $U^{\rm ex}$ (see supplementary information (SI) available online at stacks.iop.org/NJP/21/013035/mmedia) shows, that the degree of its nonlocality decreases with the decrease of the smaller mass ratio, disappearing in the limit the ratio approaches zero, when it equals the exchange energy in Heitler–London theory of the hydrogen molecule [38, 39]. This suggests, that the expansion of $U^{\rm ex}$ into a series of powers of β, the smaller mass ratio in Cu_2O, might provide a useful approximation to the exchange interaction potential

$$\frac{1}{2V}\sum_{\mathbf{q}} U^{\rm ex}(2\mathbf{s},\,\mathbf{q})\psi(\mathbf{s}+\mathbf{q}) = \int \exp[\mathrm{i}\mathbf{s}\mathbf{r}]\,\mathrm{d}^3 r$$
$$\times\left[A_0(r) + \beta\, A_1(r)\frac{\mathrm{d}}{\mathrm{d}r} + \beta^2\, A_2(r)\frac{\mathrm{d}^2}{\mathrm{d}r^2} + \beta^3\, A_3(r)\frac{\mathrm{d}^3}{\mathrm{d}r^3} + \ldots\right]\phi(r) \equiv \int \exp[\mathrm{i}\mathbf{s}\mathbf{r}]\,\mathrm{d}^3 r\mathcal{V}^{\rm ex}(r)\phi(r), \qquad (8)$$

if appropriately truncated. Here ϕ is any of s-wave functions of bare channels in real space, and functions $A_0(r)$, $A_1(r)$,... depend parametrically on β falling off exponentially at large distances. Let us take the value $\beta \approx 0.28$, which fits to commonly accepted values $_{ax} = 0.7$ nm, $E_b = 150$ meV and $\mu_x = 2.6m_0$ (m_0 is the free electron mass) of the key exciton parameters. For it we can truncate expansion (8) at the third term, and as a result, equations for the χ-function ($\chi = r\phi/4\pi$) of the background s-wave scattering and possible biexciton read

$$2(\beta-1)\beta E_b\chi_E'' + [\mathcal{U}^d(x) + F_0(x) - E]\chi_E + \beta\, F_1(x)\chi_E' + \beta^2\, F_2(x)\chi_E'' + \beta^3\, F_3(x)\chi_E''' = 0, \qquad (9)$$

$$2(\beta-1)\beta E_b\chi_b'' + [\mathcal{U}^d(x) - F_0(x) + 2\Delta - E_0]\chi_b - \beta\, F_1(x)\chi_b' - \beta^2\, F_2(x)\chi_b'' - \beta^3\, F_3(x)\chi_b''' = 0, \qquad (10)$$

with E_0 the biexciton energy, $x \equiv r/a_x$, and functions F_0, F_1, F_2, F_3 expressed in terms of functions A_0, A_1, A_2, A_3 (see SI). A change in deciding on a particular value for a key parameter entails quantitative changes in solutions for bare channels as well as their coupling, but the qualitative picture of the paraexciton scattering remains the same as presented below for $\beta = 0.28$.

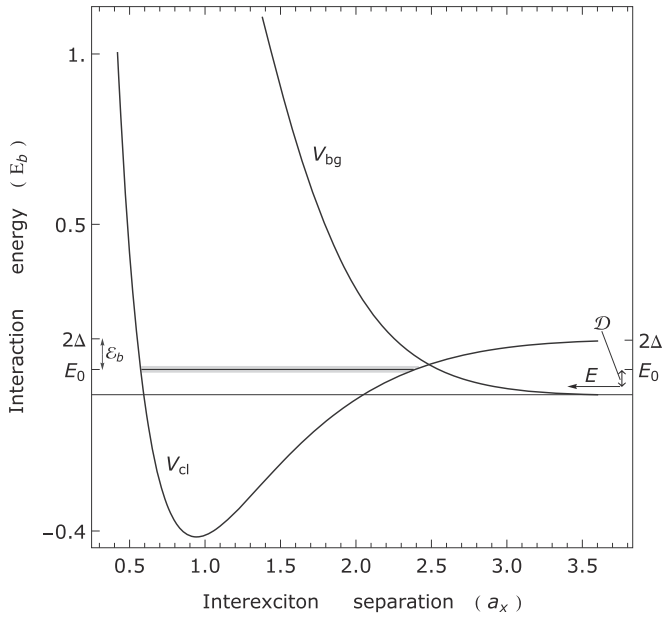

Figure 3. Approximate local equivalents of interaction potentials in bare channels. V_{bg} is presented for $E = 0$ and V_{cl}—for $E = E_0$. The biexciton is depicted by the black line in the potential well of V_{cl} with a grey strip around showing the resonance width.

On the normalization of scattering functions ϕ_E by the k scale, χ_0 has the asymptotic form $\chi_0 \approx x - a_{bg}/a_x$ [40]. By a numerical solution of equation (9) for $E = 0$ we find the background scattering length $a_{bg} \approx 1.45a_x$, which is considerably smaller than our rough hard-core estimate [35] and that computed by quantum Monte Carlo simulations for $\beta = \alpha$ [41]. The parameter determines solely the background phase shift δ_{bg} of slow paraexcitons [26]. Condition for paraexcitons to be slow depends on the range of paraexciton–paraexciton interaction potential $\mathcal{V}_{bg} = \mathcal{U}^d + \mathcal{V}^{\rm ex}$, which in its turn is defined by functions $F_0(x),\ldots,F_3(x)$. We get the range about 3_{ax}, thus paraexcitons having $k \ll (3a_x)^{-1} \approx 0.48\ \mathrm{nm}^{-1}$ are slow. To be specific, we set the point $T = 1.2$ K corresponding to $k \approx 0.06\ \mathrm{nm}^{-1}$ the upper bound of the slow paraexcitons range, but loosely, paraexcitons at temperatures of order of 2 K with $k < 0.1\ \mathrm{nm}^{-1}$ can still be considered to be slow.

As to equation (10), we find by the customary variational procedure, that it has one bound state—the biexciton with binding energy $\mathcal{E}_b = 2\Delta - E_0 \approx 13$ meV and the corresponding wave function

$$\chi_b(x) = 1.026\,61x^{10^{-6}} \exp\{-0.712\,54\exp[-1.89\exp(x - 0.952)]\}\{\exp[-1.89(x - 0.952)]\}^{0.212\,54}. \quad (11)$$

The obtained value for $\mathcal{E}_b$ is much larger than the result of Brinkman *et al* [42] and coincides with that of Huang [43]. Comparison is, however, inappropriate because in those works the exchange exciton–exciton interaction and central cell corrections have been neglected.

To have an idea of the shape of interaction potentials $\mathcal{V}_{bg}$ and $\mathcal{V}_{\rm cl} = \mathcal{U}^d - \mathcal{V}^{\rm ex}$, we perform localization procedures to obtain their approximate local equivalents [44]. Neglecting for simplicity small β^3-terms in equations (9) and (10), we turn them into usual Schrodinger equations by transformations $\chi_E(x) = T_E(x)\Phi_E(x)$ and $\chi_b(x) = T_b(x)\Phi_b(x)$, respectively. The acquired energy-dependent local equivalent potentials V_{bg} and $V_{\rm cl}$ are shown in figure 3. Their shape resembles that of the interaction potential between hydrogen atoms, respectively, in their singlet and triplet molecular states [26]. For actual interexciton distances the interaction between paraexcitons in the background channel is repulsive, whereas that between orthoexcitons in the closed channel is attractive. Being shifted upward by 2Δ, the closed channel involves the biexciton energy $E_0 = 2\Delta - \mathcal{E}_b$ (the black line inside the potential well) to be embedded in the paraexciton scattering continuum.

Effects of biexciton as a Feshbach resonance

As a perturbation, when being 'turned on' the coupling of two channels induces transitions between the biexciton and paraexciton's incoming and outgoing scattering states, which make the biexciton an intermediate state [26] for the paraexciton scattering. The biexciton is no longer a bound state, but just a scattering resonance [45], or a quasistationary state having complex energy $E_0 - i\Gamma_c/2$ with Γ_c the resonance width [26], also called the coupling strength. Consequently, the quasibiexciton has a finite lifetime $\tau = \hbar/\Gamma_c$ parameterizing its exponential decay with time. This explains the fact why the biexciton has not been detected in Cu_2O. Resonance scattering of paraexcitons on the quasibiexciton, which is schematically depicted in figure 4, happens when their

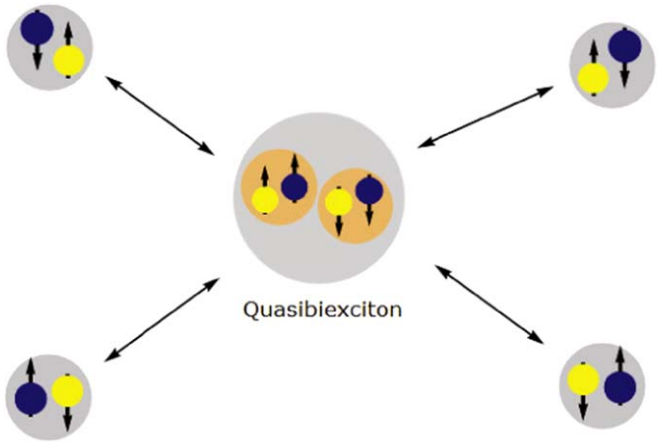

Figure 4. Resonance scattering of paraexcitons on the quasibiexciton. Two paraexcitons collide and form temporarily the quasibiexciton, which decays after some time into two paraexcitons. Two-side arrows allow one to read the schema in two directions showing that the formation and decay of the quasibiexciton take place repeatedly.

energy matches the interval of width Γ_c around E_0 (see figure 3). Such a phenomenon is long known in nuclear physics as a Feshbach resonance [46]. They have lately become an important experimental tool for controlling properties of cold atomic gases [47]. A distinctive feature of the quasibiexciton is that, it is a decaying state by itself having a width Γ_{qb} connected with all damping mechanisms—partly a consequence of the fact, that the system under consideration is not quite closed, but coupled to surroundings. In these conditions, the paraexciton scattering is an elastic collision in the presence of inelastic processes that lead to the decay of the quasibiexciton as a complex of electronic excitations. Effects of such a decaying resonance on the paraexciton scattering follow straightforwardly from nonrelativistic Breit–Wigner formulas [26]. In particular, the $\mathcal{S}$-matrix of the s-wave paraexciton scattering has the form

$$\mathcal{S}_0 = \exp[2\mathrm{i}\delta_{bg}]\left[1 + \mathrm{i}\frac{\Gamma_c}{\mathcal{D} - \mathrm{i}(\Gamma_c + \Gamma_{qb})/2}\right], \tag{12}$$

where $\mathcal{D}$ is the detuning of the scattering energy from the resonance, $\mathcal{D} = 2\Delta - \mathcal{E}_b - E$ (see figure 3). From here we have the total s-wave scattering cross section $\sigma_t = 2\pi(1 - \mathrm{Re}\,\mathcal{S}_0)/k^2$,

$$\sigma_t = \frac{\pi}{k^2}\left[4\sin^2\delta_{bg} + \frac{\Gamma_c(\Gamma_c + \Gamma_{qb})}{\mathcal{D}^2 + (\Gamma_c/2 + \Gamma_{qb}/2)^2}\cos(2\delta_{bg}) + 2\frac{\mathcal{D}\Gamma_c}{\mathcal{D}^2 + (\Gamma_c/2 + \Gamma_{qb}/2)^2}\sin 2\delta_{bg}\right]. \tag{13}$$

As seen, the coupling to the quasibiexciton causes a resonance scattering superimposed on the paraexciton background scattering. It is described by the two last terms in brackets presenting, respectively, the resonance scattering and its interference with the background scattering. They include two quasibiexciton effects. First, a paraexciton loss described by the inelastic cross section $\sigma_r = \pi(1 - |\mathcal{S}_0|^2)/k^2$, whose rate is

$$A = v\sigma_r = 4\pi\frac{\hbar^2}{\mu_x}\sqrt{\frac{6}{\mu_x E}}\frac{\Gamma_c}{2\mathcal{D}}\frac{\Gamma_{qb}}{2\mathcal{D}}\left[1 + \left(\frac{\Gamma_c}{2\mathcal{D}} + \frac{\Gamma_{qb}}{2\mathcal{D}}\right)^2\right]^{-1}, \tag{14}$$

where $v = \sqrt{6E/\mu_x}$ is the mean thermal velocity of the scattering particle with mass $\mu_x/2$. We would like to note, that no quasibound state affect higher waves, so the paraexciton loss at any temperature $T \ll 2\Delta/k_B$ is connected entirely with the s-wave quasibiexciton. Characterizing the decaying resonance, the loss rate depends on $\Gamma_{qb}/2\mathcal{D}$, along with $\Gamma_c/2\mathcal{D}$ determining the scale of Feshbach resonance effects. Let us assume, that Γ_{qb} is about two times the paraexciton decay width, $\Gamma_{qb} \approx 2\Gamma_p$. Besides a negligibly small population relaxation rate, Γ_p comprises homogeneous broadening due to the exciton–exciton and exciton–phonon scattering, Γ_{x-x} and Γ_{ph}, and inhomogeneous broadening Γ_{inh} due to fluctuations of the sample structure and applied fields. We see, that Γ_{ph} makes the paraexciton loss persistent at low densities as reported in [7, 18] and [20], and Γ_{inh} is a source of uncertainty contributing to the divergence of experimental estimates of the loss rate [12, 14]. Further, the loss rate of trapped paraexcitons depends on an external factor in the form of stress S, which reduces the ortho-para splitting, $\Delta = 12 - c_1 S + c_2 S^2$ ($c_1 \approx 2.03$ meV kbar^{-1}, $c_2 \approx 0.14$ meV kbar^{-2}) [20, 48]. Leaving aside a stress dependence of Γ_p, we expect roughly from equation (14) that A first increases with S reaching its largest value at the true resonance $\mathcal{D} = 0$, then decreases. In fact, at $T = 2$ K where $\mathcal{D} = 0$ under $S \approx 3.4$ kbar, the increase of the rate was observed for discrete stress values from 1.5 to 3.5 kbar [16].

Table 1. Denotations and abbreviations.

Exciton binding energy	E_b
Exciton effective radius	a_x
Exciton total mass and reduced mass	μ_x and μ_r
Ortho-para splitting energy	Δ
Direct exciton–exciton interaction potential	$\mathcal{U}^d$
Approximate exchange exciton–exciton interaction potential	$\mathcal{V}^{\rm ex}$
Interaction potential between paraexcitons	$\mathcal{U}^d + \mathcal{V}^{\rm ex}$
Interaction potential between orthoexcitons	$\mathcal{U}^d - \mathcal{V}^{\rm ex}$
Paraexciton scattering energy	$E = k_B T$
Paraexciton background scattering length	a_{bg}
Quasibiexciton binding energy	$\mathcal{E}_b$
Quasibiexciton energy	$E_0 = 2\Delta - \mathcal{E}_b$
Quasibiexciton resonance width (coupling strength)	Γ_c
Quasibiexciton own width	Γ_{qb}
Paraexciton energy detuning from resonance	$\mathcal{D} = E_0 - E$
Diminution of a_{bg} caused by resonance scattering	$a_{\rm res}$
Paraexciton (total) scattering length	$a = a_{bg} + a_{\rm res}$
Paraexciton elastic cross section	$\sigma_e = 4\pi a^2$
Paraexciton inelastic cross section	σ_r
Mean thermal velocity of the scattering particle	$v = (6k_B T/\mu_x)^{1/2}$
Paraexciton loss (inelastic collision) rate	$A = v\sigma_r$
Paraexciton elastic collision rate	$K = v\sigma_e$
Paraexciton broadening by exciton–exciton interaction	$\Gamma_{x-x} = \hbar n(K + A)$
Paraexciton broadening by exciton–phonon interaction	$\Gamma_{\rm ph}$
Inhomogeneous broadening	$\Gamma_{\rm inh}$
Paraexciton decay width	$\Gamma_p = \Gamma_{x-x} + \Gamma_{\rm ph} + \Gamma_{\rm inh}$
Applied stress	S
Critical stress, under which a turns its sign	S_0

The other quasibiexciton effect is characteristic of Feshbach resonances. It is a change introduced to the paraexciton–paraexciton interaction described by the elastic cross section $\sigma_e = \sigma_t - \sigma_r$. Clearly, the terms other than $4\sin^2\delta_{bg}$ and σ_r in equation (13) together present an additional interaction joining up with the background repulsive interaction between paraexcitons. Rich physics of resonance effects, whose scale is defined by the ratio between the quasibiexciton total width and detuning, is beyond the scope of this paper. In the following we confine our analysis to slow paraexcitons under moderate stress relevant to recent experiments [10–13] and also to a part of an earlier experiment by Denev and Snoke [16]. Their elastic cross section has the form

$$\sigma_e|_{ka_{bg}\ll 1} \simeq 4\pi\left\{a_{bg} - \frac{1}{k}\frac{\Gamma_c}{2\mathcal{D}}\left[1 + \left(\frac{\Gamma_c}{2\mathcal{D}} + \frac{\Gamma_p}{\mathcal{D}}\right)^2\right]^{-1}\right\}^2, \tag{15}$$

which shows the emergence of a resonance term $a_{\rm res} \propto -\Gamma_c/2\mathcal{D}$ in the paraexciton scattering length $a = a_{bg} + a_{\rm res}$ presenting an extra attractive interaction.

Quantitative estimates and interpretation of experimental results

To estimate quasibiexciton effects, we have to evaluate Γ_c and Γ_p. Stress moves the quasibiexciton position, which is already quite close to the scattering threshold in an unstressed crystal, further downwards (see figure 3). A resonance that is close to the scattering threshold has an energy-dependent width, $\Gamma_c = 2\gamma_0 k$ with γ_0 a constant [26, 40, 47]. The quantity is derived from the second-order correction to the discrete energy level caused by the coupling potential as a perturbation, $\Gamma_c = 2\pi\sum_{\mathbf{q}}[\langle\phi_0|\sqrt{3}\,\mathcal{V}^{\rm ex}|\phi_b\rangle]^2\delta(E_q - E)$ [26, 40]. Using functions χ_0, χ_b and $\mathcal{V}^{\rm ex}$ obtained in the previous subsection for computing the transition matrix element, we get $\gamma_0 \approx 7.05$ nm meV. As to Γ_p, we put $\Gamma_p \simeq \Gamma_{x-x} + \Gamma_{\rm ph}$ neglecting inhomogeneity of the strain field (see table 1). It is known, that at such low temperatures that the paraexciton energy is less than $\mu_x u^2/2$, where $u = 4.5 \times 10^5$ cm s^{-1} is the velocity of the longitudinal acoustic phonon, the paraexciton–phonon scattering is exponentially restrained [20, 49]. As a result, at $T \lesssim 2$ K $\Gamma_{\rm ph}$ is extremely small. In fact, at low densities $\Gamma_{\rm ph}$ amounts to the paraexciton decay width Γ_p that has been reported to be 80 neV at $T = 1.2$ K [50]. In strain-induced traps, Γ_p depends on stress through $\Gamma_{x-x} = \hbar n(K + A)$ ($K = 4\pi a^2 v$—the elastic collision rate), but our estimates show that for moderate stress its highest value is just of order of microelectronvolts. Under conditions of recent experiments on trapped paraexcitons in Cu_2O ($T \lesssim 2$ K, $S < 2$ kbar), we have detuning $\mathcal{D} > 3$ meV, hence $(\Gamma_p/\mathcal{D})^2$ is negligible and equations (14) and (15) give, respectively,

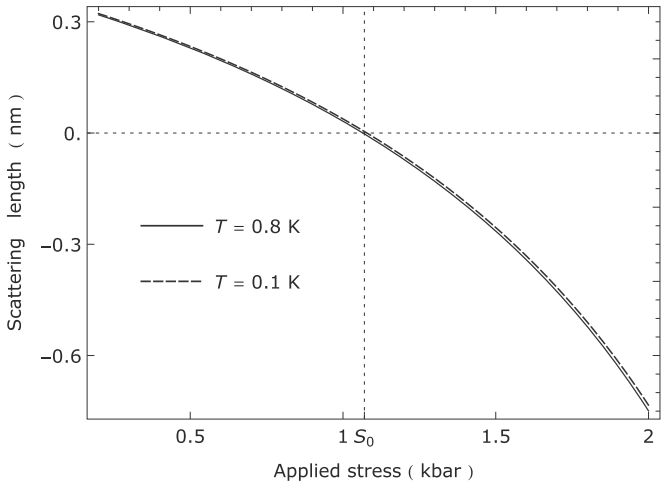

Figure 5. Stress dependence of the paraexciton scattering length.

$$a \simeq a_{bg} - \frac{\gamma_0}{\mathcal{D}}\left[1 + \left(\frac{\gamma_0 k}{\mathcal{D}}\right)^2\right]^{-1}, \quad A \simeq 4\pi\sqrt{6}\,\frac{\hbar}{\mu_x}\frac{\gamma_0}{\mathcal{D}}\frac{\Gamma_p}{\mathcal{D}}\left[1 + \left(\frac{\gamma_0 k}{\mathcal{D}}\right)^2\right]^{-1}. \tag{16}$$

One can see that the paraexciton scattering length depends on stress through the energy detuning $\mathcal{D}$. It is obvious from figure 5, where a is shown as a function of stress for two values of the temperature, that a depends little on T, but monotonically decreases with stress turning its sign at a value S_0 in a low stress range. The critical stress value is almost temperature-independent being about 1.07 kbar at $T = 0.8$ K and 1.08 kbar at $T = 0.1$ K. BEC of a trapped Bose gas with $a < 0$ is possible [51–53], but unstable leading to the condensate's collapse [54–56]. This happens when the number of condensate particles exceeds a critical number $N_{\rm cr} \approx 0.46 a_{\rm ho}/|a|$ ($a_{\rm ho}$—the mean harmonic oscillator length). For the trap with $a_{\rm ho} \approx 0.615$ μm under S=1.4 kbar at $T = 0.8$ K from [10], we get $N_{\rm cr} \approx 1200$. It seems that this number was exceeded, so the formed condensate collapsed and subsequently exploded.

Concerning the loss rate $A \propto \Gamma_p/\mathcal{D}^2$, its stress dependence is connected with that of both Γ_p and $\mathcal{D}$. Among two terms of Γ_p, Γ_{x-x} depends on stress via A (see table 1), while $\Gamma_{\rm ph}$ is stress-independent. As a matter of fact, at low temperatures the interaction of paraexcitons with phonons consists of their interaction with longitudinal acoustic phonons, which does not depend on stress, and that with transverse acoustic phonons, which is negligibly weak [57]. For $T = 1.2$ K, where $\Gamma_{\rm ph} = 80$ neV, we compute Γ_{x-x} and A by iterations in the stress range from 0.2 kbar to 2 kbar for the density reported in [10–13]. The result is shown in figures 6(a) and (b), respectively, for Γ_p and A. Including a term proportional to $K \propto a^2$, both parameters have their minimum at S_0, where $a = 0$, then begin to rise gaining steep increase when stress approaches the point 2 kbar, which is on the way to the resonance area of $\mathcal{D} \approx 0$ at $S \approx 3.5$ kbar. As mentioned earlier, the increase of A with stress under moderate and higher stress has actually been observed at $T = 2$ K [16]. Furthermore, it is important to note, that for stress $S < S_0$ the decrease of Γ_p with increasing stress, which is connected with that of K (see figure 6(a)), balances the decrease of $\mathcal{D}^2$ resulting in almost stress-independent loss rate in the low stress range up to 1.1 kilobar, as seen from figure 6(b). The rate in the whole stress range remains very low, just of order of 10^{-20} cm^3 ns^{-1}. Even if the inhomogeneous broadening raises the value by an order, it is still below the critical value 5×10^{-19} cm^3 ns^{-1} above which no BEC is possible [19]. The stress independence of the paraexciton loss rate and its low value in the low stress range have been reported in [16] and mentioned again in [17]. Concerning the relationship between the elastic and inelastic collision rates, we notice, that apart from the close vicinity of S_0, where $K < A$ (see figure 6(b), the inset), the former absolutely dominates with ratio K/A about 50. The factor is favorable for evaporative cooling of thermal paraexciton clouds [58]. As to the relationship between two terms of the paraexciton decay width, we see from the inset in figure 6(a) that near S_0 $\Gamma_{x-x} \approx 0$, so $\Gamma_{\rm ph}$ is the main term of Γ_p, whereas far from the point $\Gamma_{x-x} \approx \hbar n K$ predominates. Under stress about 1.5 kbar and higher, $\Gamma_p \approx \Gamma_{x-x}$, so A decreases with temperature as $\nu \propto T^{1/2}$. Then from the value $A \approx 5 \times 10^{-19}$ cm^3 ns^{-1} under stress 1.5 kbar at $T = 1.2$ K drawn from figure 6(b) one can infer that A is about 4×10^{-19} cm^3 ns^{-1} at $T = 0.8$ K and 2×10^{-19} cm^3 ns^{-1} at $T = 0.2$ K. These values are an order of magnitude lower than those ones reported in [12] and [13], respectively. The applied stress used in experiments of [13] is reported to be lower, than that used in experiments of [12], so the value of A must be less still. To our knowledge, so far [12] and [13] are the only works reporting values of A measured in the subkelvin temperature range. Moreover, it seems to us

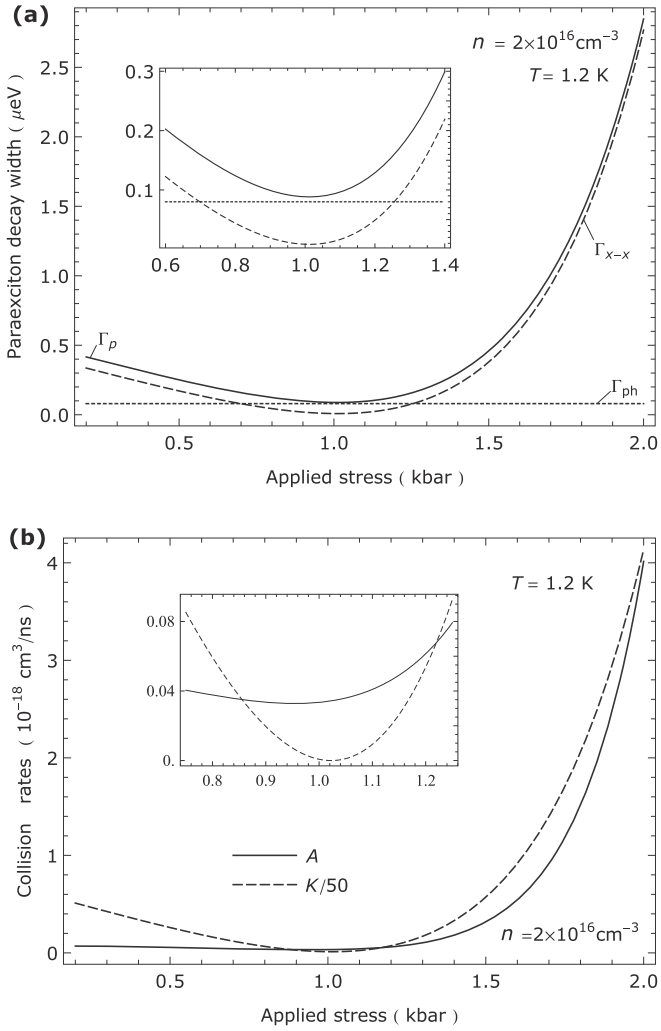

Figure 6. Stress dependence of the decay and loss parameters of slow paraexcitons (a) of the decay width and its two components, and (b) of the loss rate on the background of the fiftyfold reduced elastic collision rate.

that in experiments of [13] Stolz and his coworkers were close to the stress range that is appropriate for BEC, where $a \geqslant 0$ and the paraexciton loss is inefficient to have any effect.

Discussion

It is the analogy of excitons with atoms that has motivated the search for BEC in Cu_2O. However, the distinguishing feature is that excitons are composite entities made from charge-carriers—fermions, whose Coulomb-mediated correlations are ruled by the Pauli exclusion principle. The internal structure of excitons produces the spin-dependent exciton–exciton interaction that governs their BEC. In the case of yellow-series 1s excitons in Cu_2O, it results in the interconversion between a pair of paraexcitons with mutual repulsive interaction and that of orthoexcitons, which attract each other, leading to the two-channel character of the paraexciton–paraexciton scattering. We have described the scattering at low temperatures by means of perturbation theory. By an approximate way of calculating the nonlocal exchange exciton–exciton interaction potential, we have been able to estimate the paraexciton background scattering length a_{bg} and the binding energy $\mathcal{E}_b$ of the biexciton supported by the closed channel as well as the corresponding envelope functions. Together with the approximate exchange exciton–exciton interaction potential, these functions have enabled us to assess the coupling strength Γ_c of the biexciton and paraexciton scattering states. The coupling makes the biexciton a Feshbach resonance with its two characteristic effects—a loss of particles in the open channels and a diminution of their background scattering length, which give us clues about the mechanism of obstacles to achieving paraexciton BEC. First, the loss of paraexcitons observed in numerous experiments is elucidated, which turns out to be connected with continuing transitions of paraexciton's incoming and outgoing scattering states to the

quasibiexciton as an intermediate state. Reflecting the paraexciton's decaying nature characteristic of semiconductor electronic excitations, the loss rate is proportional to the paraexciton decay width Γ_p, which comprises of the exciton–exciton and exciton–phonon scattering widths and also the inhomogeneous broadening. The multiparameter dependence of Γ_p explains the wide divergence of experimental reports on the magnitude and temperature dependence of the paraexciton loss rate. At relatively high temperatures, when exciton–phonon scattering is effective, the rate can be high being likely the main cause of the paraexciton saturation in an unstressed crystal. However, of our interest in this paper are strain-confined paraexcitons at low temperatures. By shifting paraexciton and orthoexciton energies in different ways, stress reduces the ortho-para splitting Δ bringing the quasibiexciton closer in energy to paraexciton scattering states. This factor in general enhances quasibiexciton effects. Consequently, at some stress value S_0, the background scattering length is balanced by the diminution induced by the quasibiexciton, so $a = 0$, then it turns negative for $S > S_0$. As BEC of trapped bosons with $a < 0$ is unstable leading to the condensate's collapse, one has to use stress $S \leqslant S_0$ to create BEC of trapped paraexcitons. This stress range is appropriate for BEC still by the fact, that here the paraexciton loss rate is almost stress-independent with its value determined mainly by that of the paraexciton-phonon interaction. Therefore one can reduce the loss rate to such small values that it has no effect on BEC by lowering the temperature to the range near one Kelvin and below, where the paraexciton-phonon interaction is exponentially inhibited.

Our numerical analysis that has been done with the averaged value of the mass ratio $\beta = 0.28$ gives S_0 in the range just above one kilobar. This leads to a thought that the 'explosion' seen by Gonokami's group under stress of 1.4 kbar is connected with attractive interaction between trapped paraexcitons. The value of the critical stress is, however, just tentative. The calculation of S_0 has been relied on three parameters a_{bg}, $\mathcal{E}_b$ and Γ_c computed by using approximate interaction and coupling potentials. The mass ratio, which the shape of the potentials depends on, is uncertain because of central cell corrections. The used averaged value for β has been derived from a set of accepted values of the key exciton parameters as a result of an approximation. The last leads to errors of order of one percent in the calculated potentials, which make the values obtained for $\mathcal{E}_b$ and Γ_c to be not exact ones. Particularly about Γ_c, we would like to note, that the resonance width has been obtained from the second-order correction to the quasibiexciton energy produced by the coupling potential as a perturbation. That was a rough approximation because the exchange exciton–exciton interaction potential is not weak. The perturbation caused by this potential to quasistates of bare channels seems more complicated. Clearly, further work is needed on this question. In this context, our treatment gives just general qualitative features of collisional properties of cold paraexcitons leaving much room for quantitative reexamination by experiments as well as by other theoretical approaches.

Acknowledgments

The author would like to thank M Kuwata-Gonokami and K Yoshioka for valuable discussions, wherein initial ideas for this work were formed, and Van-Hoang Le and Nguyen Thanh Phuc for critical reading of the manuscript. The financial support from Vietnam National Foundation for Science and Technology Development (NAFOSTED) through Grant No. 103.01-2014.73 is acknowledged.

ORCID iDs

Cam Ngoc Hoang https://orcid.org/0000-0001-5607-7507

References

[1] Moskalenko S A 1962 *Fiz. Tverd. Tela* **4** 276
Moskalenko S A 1962 *Sov. Phys. Solid State* **4** 199 (Engl. transl.)
[2] Blatt J M, Boer K W and Brandt W 1962 *Phys. Rev.* **126** 1691
[3] Keldysh L V and Kozlov A N 1968 *Zh. Exsp. Teor. Fiz.* **54** 978
Keldysh L V and Kozlov A N 1968 *Sov. Phys. JETP* **27** 521 (Engl. transl.)
[4] Agekyan V T 1977 *Phys. Status Solidi* a **43** 11
[5] Mysyrowicz A, Hulin D and Antonetti A 1979 *Phys. Rev. Lett.* **43** 1123
[6] Hulin D, Mysyrowicz A and Benoit a la Guillaume C 1980 *Phys. Rev. Lett.* **45** 1970
[7] Trauernicht D P, Wolfe J P and Mysyrowicz A 1986 *Phys. Rev.* B **34** 2561
[8] Snoke D W, Wolfe J P and Mysyrowicz A 1990 *Phys. Rev. Lett.* **64** 2543
[9] Lin J-L and Wolfe J P 1993 *Phys. Rev. Lett.* **71** 1222
[10] Yoshioka K, Chae E and Kuwata-Gonokami M 2011 *Nat. Commun.* **2** 328
[11] Yoshioka K and Kuwata-Gonokami M 2012 *New J. Phys.* **14** 055024
[12] Schwartz R, Naka N, Kieseling F and Stolz H 2012 *New J. Phys.* **14** 023054

[13] Stolz H, Schwartz R, Kieseling F, Som S, Kaupsch M, Sobkowiak S, Semkat D, Naka N, Koch T and Fehske H 2012 *New J. Phys.* **14** 105007
[14] Snoke D and Kavoulakis G M 2014 *Rep. Prog. Phys.* **77** 116501
[15] O'Hara K E, Suilleabhain L O and Wolfe J P 1999 *Phys. Rev.* B **60** 10565
[16] Denev S and Snoke D W 2002 *Phys. Rev.* B **65** 085211
[17] Liu Y and Snoke D 2006 *Solid State Commun.* **140** 208
[18] Yoshioka K, Ideguchi T, Mysyrowicz A and Kuwata-Gonokami M 2010 *Phys. Rev.* B **82** 041201R
[19] Semkat D, Sobkowiak S, Schöne F, Stolz H, Koch T and Fehske H 2017 *J. Phys. B: At. Mol. Opt. Phys.* **50** 204001
[20] Trauernicht D P and Wolfe J P 1986 *Phys. Rev.* B **33** 8506
[21] Sandfort C, Brandt J, Finke C, Frohlich D, Bayer M, Stolz H and Naka N 2011 *Phys. Rev.* B **84** 165215
[22] Kavoulakis G M and Baym G 1996 *Phys. Rev.* B **54** 16625
[23] Jang J I and Wolfe J P 2006 *Phys. Rev.* B **74** 045211
[24] Wolfe J P and Jang J I 2014 *New J. Phys.* **16** 123048
[25] Schweiner F, Main J, Feldmaier M, Wunner G and Uihlein C 2016 *Phys. Rev.* B **93** 195203
[26] Landau L D and Lifshitz E M 1985 *Quantum Mechanics* (New York: Pergamon) Ch VI, XII, XVII, XVIII
[27] Koster G F, Dimmock J O, Wheeler R G and Statz H 1963 *Properties of the Thirty-two Point Groups* (Cambridge, MA: MIT Press)
[28] Hanamura E 1970 *J. Phys. Soc. Jpn.* **29** 50
[29] Hanamura E 1974 *J. Phys. Soc. Jpn.* **37** 1545
[30] Bobrysheva A I, Miglei M F and Shmiglyuk M I 1972 *Phys. Status Solidi* b **53** 71
[31] Haug H and Schmitt-Rink S 1984 *Prog. Quantum Electron.* **9** 3
[32] Nguyen B A, Hoang N C and Nguyen T D 1991 *J. Phys.: Condens. Matter* **3** 3317
[33] Hoang N C 2006 *Zh. Eksp. Teor. Fiz.* **129** 315
Hoang N C 2006 *Russian JETP* **102** 277 (Engl. transl.)
[34] Okumura S and Ogawa T 2001 *Phys. Rev.* B **65** 035105
[35] Hoang N C 1997 *Phys. Rev.* B **55** 10487
[36] Kavoulakis G M, Chang Y C and Baym G 1997 *Phys. Rev.* B **55** 7593
[37] French M, Schwartz R, Stolz H and Redmer R 2009 *J. Phys.: Condens. Matter* **21** 015502
[38] Heitler W and London F 1927 *Z. Phys.* **44** 455
[39] Kotani M, Ohno K and Kayama K 1961 *Molecule II* (Berlin: Springer) pp 1–172
[40] Timmermans E, Tommasini P, Hussein M and Kerman A 1999 *Phys. Rep.* **315** 199
[41] Shumway J and Ceperley D M 2001 *Phys. Rev.* B **63** 165209
[42] Brinkman W F, Rice T M and Bell B 1973 *Phys. Rev.* B **8** 1570
[43] Huang W T 1973 *Phys. Status Solidi* b **60** 309
[44] Coz M, Arnold L G and MacKellar A D 1970 *Ann. Phys.* **59** 219
[45] Taylor J R 1972 *Scattering Theory: The Quantum Theory on Nonrelativistic Collisions* (New York: Wiley)
[46] Feshbach H 1962 *Ann. Phys.* **19** 287
[47] Cheng C, Grimm R, Julienne P and Tiesinga E 2010 *Rev. Mod. Phys.* **82** 1225
[48] Waters R G, Pollack F H, Bruce R H and Cummins H Z 1980 *Phys. Rev.* B **21** 1665
[49] Moskalenko S A and Snoke D W 2005 *Bose–Einstein Condensation of Excitons and Biexcitons* (Cambridge: Cambridge University Press) Ch 8
[50] Brandt J *et al* 2007 *Phys. Rev. Lett.* **99** 217403
[51] Dalfovo F, Giorgini S, Pitaevskii L P and Stringari S 1999 *Rev. Mod. Phys.* **71** 463
[52] Bradley C C, Sackett C A, Tollett J J and Hulet R G 1995 *Phys. Rev. Lett.* **75** 1687
[53] Bradley C C, Sackett C A and Hulet R G 1997 *Phys. Rev. Lett.* **78** 985
[54] Ruprecht P A, Holland M J, Burnett K and Edwards M 1995 *Phys. Rev.* A **51** 4704
[55] Roberts J L *et al* 2001 *Phys. Rev. Lett.* **86** 4211
[56] Donley E A, Claussen N R, Cornish S L, Roberts J L, Cornell E A and Wieman C E 2001 *Nature* **412** 295
[57] Sobkowiak S, Semkat D and Stolz H 2014 *Phys. Rev.* B **90** 075206
[58] Tiesinga E, Moerdijk A J, Verhaar B J and Stoof H T C 1992 *Phys. Rev.* A **46** 1167R